# Enhancing Information Freshness for Coordinated Direct and Relay Transmission

Tse-Tin Chan and Haoyuan Pan

***Abstract*—This paper investigates the information freshness of relay-aided status updating in coordinated direct and relay transmission (CDRT) for the first time. Information freshness is measured by age of information (AoI), defined as the time elapsed since the generation of the last successfully received update packet. In CDRT, one sensor communicates directly with the receiver while another sensor requires the assistance of a decode-and-forward relay. Conventional CDRT is achieved via time division multiple access (TDMA) or non-orthogonal multiple access (NOMA). Interestingly, our experiments on software-defined radios (SDR) indicate that in error-prone wireless networks, TDMA-CDRT and NOMA-CDRT are not superior to each other in terms of peak AoI in all signal-to-noise ratio (SNR) regimes. Specifically, the direct sensor prefers NOMA-CDRT while the relay-aided sensor prefers TDMA-CDRT, leading to a dilemma in optimizing the peak AoI of the system. To this end, we put forth a hybrid CDRT scheme that combines TDMA and NOMA. The SDR experimental results show that the hybrid CDRT scheme not only balances the peak AoI of the direct and relay-aided sensors, but also achieves better information freshness for the whole CDRT system.**

***Index Terms*—Age of information (AoI), coordinated direct and relay transmission (CDRT), Internet of things (IoT), non-orthogonal multiple access (NOMA).**

## I. Introduction

INTERNET of things (IoT) gathers and shares information among a wide variety of smart devices, such as small sensors, wearables, actuators, and more [1]. For time-critical applications, such as autonomous vehicles, intelligent manufacturing, and smart cities, fresh sensing data must be delivered in a timely manner to reflect the observed current state. For example, suppose a sensor monitors any malfunction on an assembly line in a smart factory, failure to update the status in time could lead to severe consequences, such as production loss, component damage, or even injuries [2]. Therefore, timely information updating plays a crucial role in the IoT.

Manuscript received July 21, 2022 revised March 29, 2023; approved for publication by Ji-Woong Choi, Division 2 Editor, May 9, 2023.

This work was supported in part by the National Natural Science Foundation of China under Grant 62001298, in part by the Guangdong Basic and Applied Basic Research Foundation under Grant 2021A1515012601, in part by the Shenzhen Science and Technology Program under Grant RCBS20210609103234060, and in part by the Faculty Development Scheme under Grant UGC/FDS14/E02/21 and the Research Matching Grant Scheme from the Research Grants Council of Hong Kong.

T.-T. Chan is with the Department of Mathematics and Information Technology, The Education University of Hong Kong, Hong Kong SAR, China, email: tsetinchan@eduhk.hk.

H. Pan is with the College of Computer Science and Software Engineering, Shenzhen University, Shenzhen, 518060, China, email: hypan@szu.edu.cn.

H. Pan is the corresponding author.

Digital Object Identifier: 10.23919/JCN.2023.000022

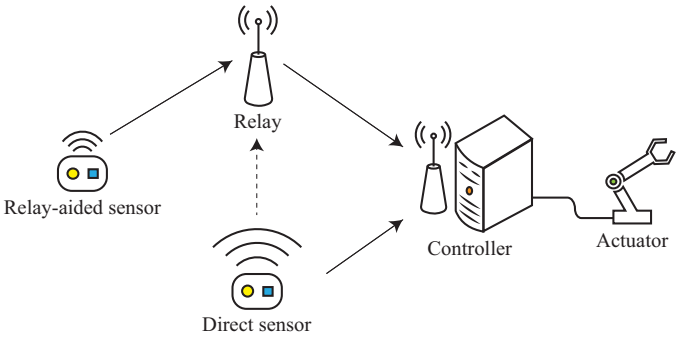


Fig. 1. An example of information update systems with CDRT.

In remote status updating, some sensors can be connected directly to the receiver wirelessly. They are referred to as direct sensors in this paper. However, some small sensors, especially those powered by batteries or placed far away from the receiver, may not be able to communicate directly with the receiver. Therefore, a relay can be used to forward status updates to the receiver [3]. We refer to these sensors as relay-aided sensors. This paper considers the coexistence of direct and relay-aided communications, which is also referred to as coordinated direct and relay transmission (CDRT) [4], as shown in Fig. 1. We design communication schemes for information update systems with CDRT. In particular, we focus on one sensor of each type, which can be easily extended to the case of multiple sensors. For example, multiple relay-aided sensors can communicate with the relay using time division multiple access (TDMA), frequency division multiple access (FDMA), etc. The relay then forwards the aggregate packets to the receiver [5].

In this paper, we focus on enhancing the *information freshness* in CDRT-enabled information update systems. Since conventional metrics, such as throughput and latency, cannot characterize the information freshness, we adopt the newly proposed performance metric: *Age of information* (AoI) [6], [7]. In contrast to latency, which measures only the time required to deliver a packet, AoI is defined as the time elapsed since the most recently received packet was generated, i.e., how fresh the latest received packet is at the current moment [8]. In recent years, AoI has been extensively investigated by various studies [8]–[14]. Early work on AoI focused on queue management schemes [7], [9], [10] and packet scheduling schemes [11]–[13]. We refer readers to recent research on AoI in the survey [14].

Nevertheless, there are no studies on the AoI performance of CDRT so far. CDRT was first considered in [4] and then



1229-2370/23/$10.00 © 2023 KICS

often worked with non-orthogonal multiple access (NOMA) to improve network performance. NOMA serves multiple users at the same resource (e.g., time, frequency, coding, etc.). It improves spectral efficiency and throughput compared with conventional orthogonal multiple access (OMA) schemes (e.g., TDMA and FDMA) [15]. Besides performance improvements, the literature showed that NOMA could effectively support large-scale connectivity, which is a prominent feature of the IoT communications [16]. Reference [17] first studied NOMA-based CDRT (NOMA-CDRT) to improve the spectral efficiency in the two-user downlink case. Then, [18] analyzed the two-user uplink case in terms of the ergodic sum capacity (ESC), and [19] studied a multi-relay scheme to improve the system performance in terms of outage probability. Recently, [20] studied the impact of full- and half-duplex relaying on the outage probability and ESC, and practical applications of NOMA-CDRT were considered in [21], [22].

As far as information freshness is concerned, whether NOMA still outperforms OMA in AoI performance for CDRT requires thorough investigation. Prior work showed that higher throughput does not always lead to lower AoI [23]. Moreover, as information freshness is critical in IoT communications, improving the AoI performance of CDRT deserves an in-depth study. This paper attempts to fill this research gap and has the following three main contributions:

1) We are the first to investigate the AoI performance of CDRT in information update systems. Specifically, we derive and compare the average peak AoI of TDMA-based CDRT (TDMA-CDRT) and NOMA-CDRT schemes. Previous studies, such as [18], [22], have shown that NOMA-CDRT has a significant performance improvement over TDMA-CDRT in terms of conventional metrics (e.g., ESC). By contrast, our experimental results using software-defined radios (SDR) show that when AoI is considered, TDMA-CDRT and NOMA-CDRT do not outperform each other in all signal-to-noise ratio (SNR) regimes. Furthermore, direct sensors prefer NOMA-CDRT, while relay-aided sensors prefer TDMA-CDRT in error-prone wireless networks.
2) We put forth a hybrid CDRT scheme that leverages TDMA-CDRT and NOMA-CDRT. Depending on the different order of the OMA and NOMA transmissions, the two possible variations are called NOMA-OMA-CDRT and OMA-NOMA-CDRT, respectively. The hybrid CDRT scheme aims to strike a balance between direct and relay-aided transmissions because both carry important information updates for remote status monitoring.
3) We are the first to demonstrate the practical feasibility of CDRT for updating sensing data with AoI requirements through SDR experiments, which is amendable to real IoT systems. The experimental results on SDR show that the proposed hybrid CDRT scheme not only balances the AoI performance of direct and relay-aided transmissions, but also achieves a lower average peak AoI of the network compared to TDMA-CDRT and NOMA-CDRT, especially when the sensor-relay or relay-receiver link is poor.

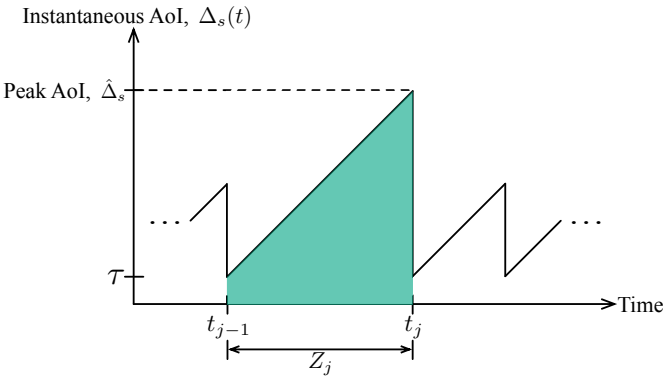


Fig. 2. An example of the instantaneous AoI of a sensor in CDRT, $\Delta(t)$.

## II. Preliminaries

This section describes the general system setup and derives a unified expression of the average peak AoI for different CDRT models. We assume that the sensors periodically send monitoring data to the receiver and that each node shares the same bandwidth. We consider a generate-at-will model where a status update packet is generated whenever the sensor has the opportunity to send it. In other words, queuing delay is not considered in this paper. When the packet decoding fails, the receiving node discards the corrupted packet without sending any feedback.

In the CDRT-based information update system shown in Fig. 1, the controller wants to receive packets from the direct and relay-aided sensors as fresh as possible. To quantify the information freshness, the instantaneous AoI of the direct sensor at time $t$ is defined as

$$\Delta_{\mathrm{d}}(t) \triangleq t - U_{\mathrm{d}}(t), \tag{1}$$

where $U_d(t)$ is the generation time of the latest successfully received packet from the direct sensor [8].

In this paper, we study the *peak AoI* performance of different CDRT schemes, which measures the AoI value reached just before the successful delivery of the update packet. Then, the time-average peak AoI of the direct sensor is denoted by $\overline{\Delta}_{\mathrm{d}}$. Similarly, the instantaneous and average peak AoI of the relay-aided sensor can be defined by replacing the subscript "d" with "r", i.e., $\Delta_{\mathrm{r}}(t)$ and $\overline{\Delta}_{\mathrm{r}}$, respectively. The peak AoI of the network, $\overline{\Delta}$, is the average of $\overline{\Delta}_{\mathrm{d}}$ and $\overline{\Delta}_{\mathrm{r}}$, i.e., $\overline{\Delta} \triangleq (\overline{\Delta}_{\mathrm{d}} + \overline{\Delta}_{\mathrm{r}})/2$.

Let us denote by $\tau$ the time required for the controller to successfully receive a packet from the sensor since the packet was generated, and $\tau_j$ corresponds to the $j$th successful update. For example, the relay-aided sensor has a larger $\mathbb{E}[\tau]$ than the direct sensor due to the two hops. Fig. 2 shows an illustrative example of the instantaneous AoI of a sensor (i.e., the direct or relay-aided sensor), denoted by $\Delta_s(t)$ and $s \in \{d, r\}$. We assume that the $(j-1)$th and $j$th successful updates occur at times $t_{j-1}$ and $t_j$, respectively. The instantaneous AoI of the packet drops from $\hat{\Delta}_s$ (the peak AoI) to $\tau_j$ when the controller successfully receives the $j$th update. Then $\Delta_s(t)$ increases linearly with time until the next successful update. We use $Z$ to denote the time between two consecutive successful updates and $Z_j$ to denote the time between the $(j-1)$th and $j$th successful updates.

Using Fig. 2, we can derive the average peak AoI of the direct or relay-aided sensor, $\overline{\Delta}_s, s \in \{d, r\}$, in CDRT as

$$\overline{\Delta}_s \triangleq \lim_{J\to\infty} \frac{1}{J}\sum_{j=1}^{J}(\tau_{j-1} + Z_j) = \mathbb{E}[\tau] + \mathbb{E}[Z], \tag{2}$$

which means that the average peak AoI is affected by the transmission time from the sensor to the controller ($\tau$) and the time interval between two consecutive successful updates ($Z$).

## III. Average Peak AoI of TDMA-CDRT and NOMA-CDRT

This section derives the average peak AoI of TDMA-CDRT and NOMA-CDRT. Our SDR experimental results in Section V show that the direct sensor prefers NOMA-CDRT while the relay-aided sensor prefers TDMA-CDRT in error-prone wireless networks, resulting in a dilemma of which scheme should be used to reduce the average peak AoI of the network.

### A. TDMA-CDRT

In TDMA-CDRT, nodes send packets one by one in orthogonal time slots, as shown in Fig. 3. We use $T$ to denote the duration of each time slot in the CDRT schemes. The relay-aided sensor first transmits its sensed data to the relay, which then forwards it to the controller in the subsequent time slot. After that, the direct sensor sends its packet to the controller. The nodes continue this transmission order thereafter.

Since (2) shows that the average peak AoI is affected by $\tau$ and $Z$, we now derive $\mathbb{E}[\tau]$ and $\mathbb{E}[Z]$ to compute the average peak AoI of TDMA-CDRT. We denote the transmission time from the direct and relay-aided sensors to the controller by $\tau_{\mathrm{d}}^{\mathrm{TD}}$ and $\tau_{\mathrm{r}}^{\mathrm{TD}}$, respectively. Throughout this paper, symbols in other CDRT schemes are defined similarly by replacing the superscript "TD", so we omit repetitive definitions in the rest of the paper. Denote the time interval between two consecutive successful updates of the direct and relay-aided sensors in TDMA-CDRT by $Z_{\mathrm{d}}^{\mathrm{TD}}$ and $Z_{\mathrm{r}}^{\mathrm{TD}}$, respectively. According to Fig. 3, we can deduce $\mathbb{E}[\tau_{\mathrm{d}}^{\mathrm{TD}}] = T$ and $\mathbb{E}[\tau_{\mathrm{r}}^{\mathrm{TD}}] = 2T$. That is, the relay-aided sensor requires one more time slot due to the two-hop transmission.

We next compute $\mathbb{E}[Z]$. Let $X_{\mathrm{d}}^{\mathrm{TD}}$ ($X_{\mathrm{r}}^{\mathrm{TD}}$) represent the number of update packets transmitted by the direct sensor (the relay-aided sensor) between two consecutive successful decodings at the controller. From Fig. 3, it is easy to figure out that $Z_{\mathrm{d}}^{\mathrm{TD}} = 3TX_{\mathrm{d}}^{\mathrm{TD}}$ and $Z_{\mathrm{r}}^{\mathrm{TD}} = 3TX_{\mathrm{r}}^{\mathrm{TD}}$. This is because the direct sensor (the relay-aided sensor) transmits packets every $3T$ time interval, and the packet is successfully decoded after $X_{\mathrm{d}}^{\mathrm{TD}}$ ($X_{\mathrm{r}}^{\mathrm{TD}}$) transmissions.

For theoretical analysis, when a receiver is receiving only one packet, we assume that the successful reception probability of that packet is $p^{\mathrm{O}} \in [0, 1]$. In other words, in TDMA-CDRT, the successful reception probabilities of packets from the direct sensor to the controller ($P_{\mathrm{d}}^{\mathrm{TD}}$), from the relay-aided sensor to the relay ($P_{\mathrm{r1}}^{\mathrm{TD}}$), and from the relay to the controller ($P_{\mathrm{r2}}^{\mathrm{TD}}$) are all equal to $p^{\mathrm{O}}$. Extensions to different successful reception probabilities are straightforward.

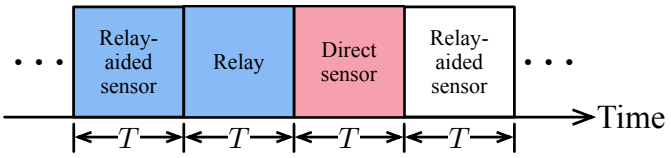


Fig. 3. TDMA-CDRT system model.

Considering the direct sensor, $X_{\mathrm{d}}^{\mathrm{TD}}$ is a geometric random variable with parameter $p^{\mathrm{O}}$. Then we have the expected values $\mathbb{E}[X_{\mathrm{d}}^{\mathrm{TD}}] = 1/P_{\mathrm{d}}^{\mathrm{TD}} = 1/p^{\mathrm{O}}$. According to (2), the average peak AoI of the direct sensor in TDMA-CDRT is computed by

$$\overline{\Delta}_{\mathrm{d}}^{\mathrm{TD}} = \mathbb{E}[\tau_{\mathrm{d}}^{\mathrm{TD}}] + \mathbb{E}[Z_{\mathrm{d}}^{\mathrm{TD}}] = T\left(\frac{3}{p^{\mathrm{O}}} + 1\right). \tag{3}$$

Regarding the relay-aided sensor, since two hops are needed, the overall successful reception probability (i.e., the success probability of conveying a packet from the source to the controller) is $P_{\mathrm{r}}^{\mathrm{TD}} = P_{\mathrm{r1}}^{\mathrm{TD}} P_{\mathrm{r2}}^{\mathrm{TD}} = (p^{\mathrm{O}})^2$. Hence, $\mathbb{E}[X_{\mathrm{r}}^{\mathrm{TD}}] = 1/P_{\mathrm{r}}^{\mathrm{TD}} = 1/(p^{\mathrm{O}})^2$. As with the direct sensor, the average peak AoI of the relay-aided sensor in TDMA-CDRT is

$$\overline{\Delta}_{\mathrm{r}}^{\mathrm{TD}} = \mathbb{E}[\tau_{\mathrm{r}}^{\mathrm{TD}}] + \mathbb{E}[Z_{\mathrm{r}}^{\mathrm{TD}}] = T\left(\frac{3}{(p^{\mathrm{O}})^2} + 2\right). \tag{4}$$

As a result, the average peak AoI of TDMA-CDRT is

$$\begin{aligned}\overline{\Delta}^{\mathrm{TD}} &= \frac{1}{2}\left(\overline{\Delta}_{\mathrm{d}}^{\mathrm{TD}} + \overline{\Delta}_{\mathrm{r}}^{\mathrm{TD}}\right) \\ &= \frac{1}{2}\left(T\left(\frac{3}{p^{\mathrm{O}}} + 1\right) + T\left(\frac{3}{(p^{\mathrm{O}})^2} + 2\right)\right) \\ &= \frac{3T}{2}\left(\frac{1}{(p^{\mathrm{O}})^2} + \frac{1}{p^{\mathrm{O}}} + 1\right).\end{aligned} \tag{5}$$

Note that the successful reception probabilities (e.g., $p^{\mathrm{O}}$) depend on various factors, such as SNR and channel model (link gain). The results derived in this paper can be applied to a wide range of wireless scenarios by using appropriate models of successful reception probabilities. In addition, to provide a clear view of the performance of different schemes in a real wireless communication environment, experiments using universal software radio peripheral (USRP) are conducted to demonstrate the peak AoI performance of the schemes in Section V.

### B. NOMA-CDRT

We can see that in TDMA-CDRT, if all the transmissions are successful, it takes three time slots for the controller to receive one packet from each sensor. In contrast, as we will see in NOMA-CDRT, only two time slots are needed to deliver two packets from the direct sensor and one packet from the relay-aided sensor to the controller. In this subsection, as in the TDMA-CDRT part, we derive the average peak AoI of NOMA-CDRT after obtaining $\mathbb{E}[\tau]$ and $\mathbb{E}[Z]$.

As shown in Fig. 4, NOMA-CDRT repeats the transmission sequence every two time slots. In the first time slot, the relay-aided sensor transmits its packet to the relay, and the direct sensor delivers its packet to the controller. Since these sensors share the same communication resources, the relay also receives the signals from the direct sensor. The relay

tries to decode the packet from the relay-aided sensor by NOMA (i.e., multiuser decoding; see Section V).

In the second time slot, there are two possible cases. If the packet from the relay-aided sensor is successfully decoded at the relay, the packet is forwarded to the controller. Meanwhile, the direct sensor also transmits its packet to the controller. The controller tries to decode the two packets as the relay does in the first time slot. In the other case, if the packet from the relay-aided sensor fails to be decoded at the relay, only the direct sensor transmits its packet to the controller.

According to Fig. 4, we can deduce $\mathbb{E}[\tau_{\rm d}^{\rm NO}] = T$ and $\mathbb{E}[\tau_{\rm r}^{\rm NO}] = 2T$ in NOMA-CDRT, because one time slot is needed to convey the packet from the direct sensor while two time slots are required for the relay-aided sensor. Furthermore, it is easy to find that $\mathbb{E}[Z_{\rm d}^{\rm NO}] = T\mathbb{E}[X_{\rm d}^{\rm NO}]$ and $\mathbb{E}[Z_{\rm r}^{\rm NO}] = 2T\mathbb{E}[X_{\rm r}^{\rm NO}]$ based on Fig. 4.

The derivations about $X_{\rm d}^{\rm NO}$ and $X_{\rm r}^{\rm NO}$ based on the successful reception probabilities are more complicated in NOMA-CDRT. For theoretical analysis, we assume that if the receiver tries to decode two simultaneous incoming packets by NOMA, the successful reception probability of each packet is $p^{\rm N} \in [0, 1]$. Note that in general, $p^{\rm N} < p^{\rm O}$ under the same received SNR.

In the first time slot, the successful reception probability of the packet from the direct sensor to the controller ($P_{\rm d,1}^{\rm NO}$) is $p^{\rm O}$. Moreover, the successful reception probability of the packet from the relay-aided sensor to the relay ($P_{\rm r1}^{\rm NO}$) is $p^{\rm N}$ because the packet from the direct sensor interferes at the relay.

In the second time slot, there are two possible cases:

- Case I, with probability $P_{\rm r1}^{\rm NO}$: the packet from the relay-aided sensor is successfully decoded at the relay in the first time slot. The successful reception probabilities of packets from the direct sensor ($P_{\rm d,2a}^{\rm NO}$) and the relay ($P_{\rm r2}^{\rm NO}$), respectively, to the controller in Case I are $p^{\rm N}$.
- Case II, with probability $(1 - P_{\rm r1}^{\rm NO})$: the packet from the relay-aided sensor fails to be decoded by the relay in the first time slot. Then the successful reception probability of the packet from the direct sensor to the controller in Case II ($P_{\rm d,2b}^{\rm NO}$) is $p^{\rm O}$.

Therefore, in the second time slot, the overall successful reception probability of the packet from the direct sensor to the controller ($P_{\rm d,2}^{\rm NO}$) is

$$\begin{aligned} P_{\rm d,2}^{\rm NO} &= P_{\rm r1}^{\rm NO} P_{\rm d,2a}^{\rm NO} + (1 - P_{\rm r1}^{\rm NO}) P_{\rm d,2b}^{\rm NO} \\ &= p^{\rm N} p^{\rm N} + (1 - p^{\rm N}) p^{\rm O}. \end{aligned} \tag{6}$$

Moreover, the overall successful reception probability of the packet from the relay-aided sensor to the controller is

$$P_{\rm r}^{\rm NO} = P_{\rm r1}^{\rm NO} P_{\rm r2}^{\rm NO} = (p^{\rm N})^2. \tag{7}$$

As a result, for the relay-aided sensor, we have the expected value $\mathbb{E}[X_{\rm r}^{\rm NO}] = 1/P_{\rm r}^{\rm NO} = 1/(p^{\rm N})^2$. For the direct sensor, we have the expected value $\mathbb{E}[X_{\rm d}^{\rm NO}] = \frac{2}{P_{\rm d,1}^{\rm NO} + P_{\rm d,2}^{\rm NO}} = \frac{2}{2p^{\rm O} - p^{\rm O}p^{\rm N} + (p^{\rm N})^2}$. Since the direct sensor has different successful reception probabilities in the first and second time slots, the derivation of $\mathbb{E}[X_{\rm d}^{\rm NO}] = \frac{2}{P_{\rm d,1}^{\rm NO} + P_{\rm d,2}^{\rm NO}}$ involves a series of steps, which can be found in Appendix A.

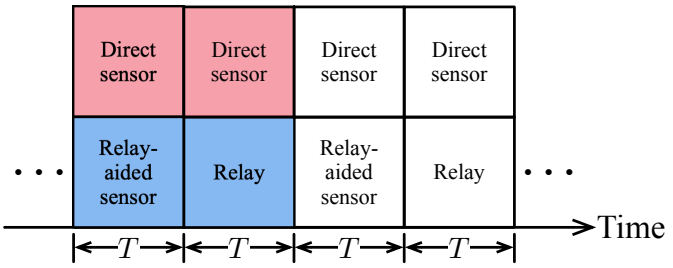


Fig. 4. NOMA-CDRT system model.

The average peak AoI of the direct sensor in NOMA-CDRT is then computed by

$$\overline{\Delta}_{\rm d}^{\rm NO} = \mathbb{E}[\tau_{\rm d}^{\rm NO}] + \mathbb{E}[Z_{\rm d}^{\rm NO}] = T\left(\frac{2}{2p^{\rm O} - p^{\rm O}p^{\rm N} + (p^{\rm N})^2} + 1\right), \tag{8}$$

while the average peak AoI of the relay-aided sensor in NOMA-CDRT is

$$\overline{\Delta}_{\rm r}^{\rm NO} = \mathbb{E}[\tau_{\rm r}^{\rm NO}] + \mathbb{E}[Z_{\rm r}^{\rm NO}] = T\left(\frac{2}{(p^{\rm N})^2} + 2\right). \tag{9}$$

Hence, the average peak AoI of NOMA-CDRT is

$$\begin{aligned} \overline{\Delta}^{\rm NO} &= \frac{1}{2}\left(\overline{\Delta}_{\rm d}^{\rm NO} + \overline{\Delta}_{\rm r}^{\rm NO}\right) \\ &= \frac{1}{2}\left(T\left(\frac{2}{2p^{\rm O} - p^{\rm O}p^{\rm N} + (p^{\rm N})^2} + 1\right) + T\left(\frac{2}{(p^{\rm N})^2} + 2\right)\right) \\ &= \frac{T}{2}\left(\frac{2}{2p^{\rm O} - p^{\rm O}p^{\rm N} + (p^{\rm N})^2} + \frac{2}{(p^{\rm N})^2} + 3\right). \end{aligned} \tag{10}$$

Prior studies [18], [22] showed that NOMA-CDRT achieves higher throughput than TDMA-CDRT does. Interestingly, as a preview, our SDR experiments in Section V find that although $\overline{\Delta}_{\rm d}^{\rm NO} < \overline{\Delta}_{\rm d}^{\rm TD}$ in all SNR regimes, $\overline{\Delta}_{\rm r}^{\rm NO} > \overline{\Delta}_{\rm r}^{\rm TD}$ in the low to medium SNR regime. In other words, the direct sensor prefers NOMA-CDRT, while the relay-aided sensor prefers TDMA-CDRT in the low to medium SNR regime. For a comprehensive graphical representation of the average peak AoI for different schemes and their performance comparisons, please refer to Section V.

As a result, for the whole CDRT network, $\overline{\Delta}^{\rm TD}$ and $\overline{\Delta}^{\rm NO}$ are not lower than each other in all SNR regimes. We are faced with a dilemma between these two CDRT schemes. Compared to TDMA-CDRT, the direct sensor in NOMA-CDRT can send more packets in the same period, which may lead to a lower average peak AoI of the system because of the smaller time interval between updates. However, NOMA-CDRT also reduces the successful reception probability when a receiver receives packets from more than one source simultaneously. If a packet fails to be decoded, the controller has to wait longer for the next update, which may result in a higher average peak AoI of the system. Hence, the following section puts forth a hybrid CDRT scheme to address this dilemma.

## IV. Average Peak AoI of NOMA-OMA-CDRT

This section presents the hybrid CDRT scheme with two variations: NOMA-OMA-CDRT and OMA-NOMA-CDRT.

The hybrid CDRT scheme balances the needs of the direct and relay-aided sensors (i.e., keeping the average peak AoI of both sensors low), as they both convey essential information updates. Furthermore, hybrid CDRT can maintain a relatively low average peak AoI of the whole network in all SNR regimes.

We first introduce NOMA-OMA-CDRT as illustrated in Fig. 5. In each of the two time slots, the transmission process starts with NOMA, followed by OMA. In the first time slot, the direct and relay-aided sensors send their status packets to the controller and the relay, respectively. As in NOMA-CDRT, the relay attempts to decode the packet of the relay-aided sensor from the interfering signals by NOMA. If the decoding is successful, only the relay forwards the packet to the controller in the second time slot. Unlike NOMA-CDRT, the direct sensor here does not transmit in the second time slot to prevent impairing the successful reception probability of the packet from the relay.

The average peak AoI of NOMA-OMA-CDRT can be derived similarly as in the previous section. Considering the direct sensor, we see from Fig. 5 that it needs one time slot to transmit its packets to the controller, hence $\mathbb{E}[\tau_{\mathrm{d}}^{\text{NO-O}}] = T$. Moreover, the direct sensor transmits its packets once every two time slots, therefore $\mathbb{E}[Z_{\mathrm{d}}^{\text{NO-O}}] = \mathbb{E}[2TX_{\mathrm{d}}^{\text{NO-O}}] = 2T\mathbb{E}[X_{\mathrm{d}}^{\text{NO-O}}]$. As the direct sensor communicates with the controller without interference, the successful reception probability of its packet, $P_{\mathrm{d}}^{\text{NO-O}}$, is $p^{\mathrm{O}}$. We then have $\mathbb{E}[X_{\mathrm{d}}^{\text{NO-O}}] = 1/P_{\mathrm{d}}^{\text{NO-O}} = 1/p^{\mathrm{O}}$. Hence, the average peak AoI of the direct sensor can be found by

$$\overline{\Delta}_{\mathrm{d}}^{\text{NO-O}} = \mathbb{E}[\tau_{\mathrm{d}}^{\text{NO-O}}] + \mathbb{E}[Z_{\mathrm{d}}^{\text{NO-O}}] = T\left(\frac{2}{p^{\mathrm{O}}} + 1\right). \tag{11}$$

Likewise, considering the relay-aided sensor, Fig. 5 shows that it takes every two time slots to deliver an update packet to the controller, therefore we have $\mathbb{E}[\tau_{\mathrm{r}}^{\text{NO-O}}] = 2T$ and $\mathbb{E}[Z_{\mathrm{r}}^{\text{NO-O}}] = 2T\mathbb{E}[X_{\mathrm{r}}^{\text{NO-O}}]$. In the first hop, the relay tries to decode the packet from the superposed signal by NOMA, therefore the successful reception probability of the packet from the relay-aided sensor to the relay, $P_{\mathrm{r1}}^{\text{NO-O}}$, is $p^{\mathrm{N}}$. In the second hop, as there is no interfering signal, the successful reception probability from the relay to the controller, $P_{\mathrm{r2}}^{\text{NO-O}}$, is $p^{\mathrm{O}}$. Since the update is successful if there are no errors in both hops, the overall successful reception probability of the packet is $P_{\mathrm{r}}^{\text{NO-O}} = P_{\mathrm{r1}}^{\text{NO-O}} P_{\mathrm{r2}}^{\text{NO-O}}$. In other words, we can derive that $\mathbb{E}[X_{\mathrm{r}}^{\text{NO-O}}] = 1/P_{\mathrm{r}}^{\text{NO-O}} = 1/p^{\mathrm{O}}p^{\mathrm{N}}$. Then the average peak AoI of the relay-aided sensor can be found by

$$\overline{\Delta}_{\mathrm{r}}^{\text{NO-O}} = \mathbb{E}[\tau_{\mathrm{r}}^{\text{NO-O}}] + \mathbb{E}[Z_{\mathrm{r}}^{\text{NO-O}}] = T\left(\frac{2}{p^{\mathrm{O}}p^{\mathrm{N}}} + 2\right). \tag{12}$$

As a result, the average peak AoI of NOMA-OMA-CDRT is

$$\begin{aligned}\overline{\Delta}^{\text{NO-O}} &= \frac{1}{2}\left(\overline{\Delta}_{\mathrm{d}}^{\text{NO-O}} + \overline{\Delta}_{\mathrm{r}}^{\text{NO-O}}\right) \\ &= \frac{1}{2}\left(T\left(\frac{2}{p^{\mathrm{O}}} + 1\right) + T\left(\frac{2}{p^{\mathrm{O}}p^{\mathrm{N}}} + 2\right)\right) \\ &= T\left(\frac{1}{p^{\mathrm{O}}p^{\mathrm{N}}} + \frac{1}{p^{\mathrm{O}}} + \frac{3}{2}\right).\end{aligned} \tag{13}$$

OMA-NOMA-CDRT is similar to NOMA-OMA-CDRT, and the main difference is that the former starts with OMA and then NOMA. In other words, only the relay-aided sensor sends in the first time slot, and the direct sensor sends in the second time slot in OMA-NOMA-CDRT. We refer the readers to Appendix B for the detailed computation of the average peak AoI of OMA-NOMA-CDRT. The analysis is similar to that of NOMA-CDRT, in which there are two possibilities depending on the decoding outcome at the relay in the first time slot. The experimental results in the next section compare the average peak AoI performance between NOMA-OMA-CDRT and OMA-NOMA-CDRT.

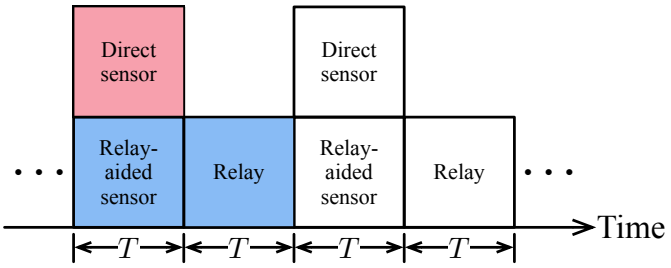

Fig. 5. NOMA-OMA-CDRT system model.

## V. Experimental Evaluation

### A. Experimental Setup

We conduct real experiments on software-defined radios (SDR) to evaluate the average peak AoI performance of different CDRT schemes. Our experiments are performed on the USRP hardware (USRP N210 with SBX daughterboards) [24] and the GNU radio software [25] with the UHD hardware driver. Each node in the CDRT is a USRP connected to a computer via an Ethernet cable. The wireless experiments operate at a center frequency of 2.185 GHz and a bandwidth of 5 MHz. In addition, BPSK modulation and the standard rate-1/2 $[133, 171]_8$ convolutional code defined in the 802.11 standards are used.

We employ a trace-driven simulation approach to evaluate the average peak AoI performances of different CDRT schemes. Specifically, we first obtain the PHY-layer decoding outcomes. We perform controlled experiments for different received SNRs (from 7 dB to 10.5 dB). For example, at each SNR, the direct sensor sends a large number of packets to the receiver (i.e., 2000 packets in our experiments), and the decoding results of different slots are recorded. Similarly, in the case of simultaneous transmissions, the receiver (the relay or the controller) sends beacon frames to trigger synchronized transmissions of the two transmitters. The NOMA decoding outcomes at the receivers are gathered. Notice that the SNRs of the two simultaneously transmitting sensors could be different. We consider both SNR-balanced and SNR-imbalanced scenarios, which will be presented in the next subsection.

To implement the NOMA decoder, instead of successive decoding as in the conventional successive interference cancellation (SIC) decoder, this paper uses a non-iterative multiuser decoding (MUD) decoder [26] to recover the two users' packets in parallel. Specifically, the received superposed signals are passed through an MUD demodulator. The MUD decoder

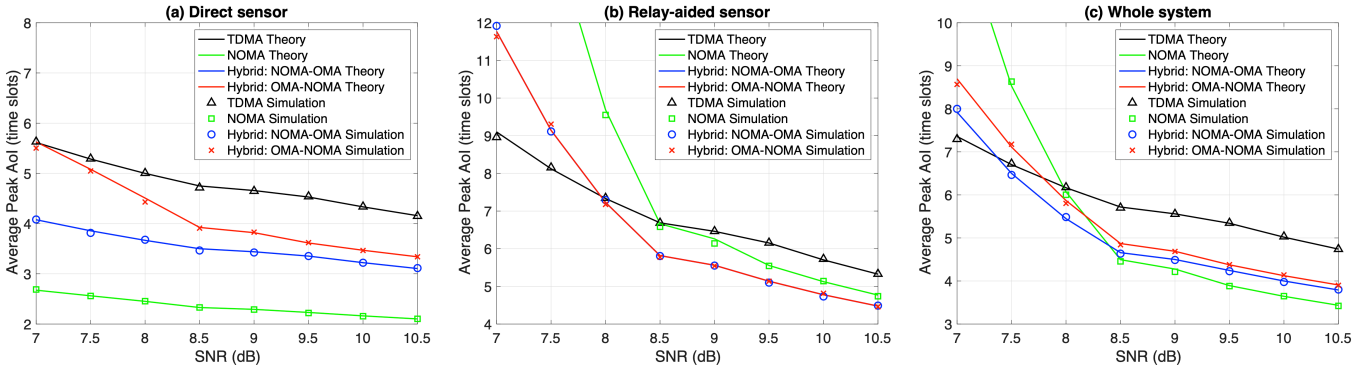


Fig. 6. SDR experimental results for the average peak AoI of (a) the direct sensor, (b) the relay-aided sensor, and (c) the whole system under different CDRT schemes with the SNR-balanced scenario.

adopts the maximum a posteriori (MAP) algorithm to compute the soft information of each channel-coded bit transmitted simultaneously by the two nodes. The soft information is then fed to two conventional point-to-point Viterbi decoders (i.e., the same decoder used for single-user transmissions) to recover the packet from each of the two nodes.

We generate traces based on the collected PHY-layer decoding outcomes to drive our AoI simulations for different CDRT schemes, from which we compute the instantaneous AoI and then the average peak AoI. In addition to the simulation results, we also present the theoretical results. We compute the successful packet reception probabilities from the decoding result statistics and then substitute them into the AoI formulas for different CDRT schemes (e.g., (3)–(5) for TDMA-CDRT) to compute the theoretical average peak AoI.

### B. Experimental Results

We first consider an SNR-balanced scenario where each link in the CDRT has the same SNR at the receiver, ranging from 7 dB to 10.5 dB, as shown in Fig. 6. For example, in NOMA-CDRT, when the direct and relay-aided sensors transmit simultaneously in the first time slot, the received SNRs of both sensors at the relay are the same. In addition, the SNR of the direct sensor at the controller is the same as that at the relay. We use an SNR-balanced scenario to validate our theoretical analysis of the average peak AoI. More importantly, a simpler setting highlights the key differences among different CDRT schemes.

As shown in Fig. 6, the simulation results corroborate with the theoretical results, except that there is a small gap for the CDRT schemes with NOMA. This is because, in our theoretical analysis, we assume that the NOMA receiver decodes each sensor's packet with success probability $p^{\mathrm{N}}$, and the success probability of decoding both sensors' packets is $(p^{\mathrm{N}})(p^{\mathrm{N}}) = (p^{\mathrm{N}})^2$. This assumption considers the decoding events of the two sensors' packets to be independent. However, in practice, the successful decodings of the two packets are usually correlated in our MAP-based MUD decoder because the MUD demodulator computes the channel-coded soft bits of the two users' symbols simultaneously from the superposed signals. Therefore, the actual probability of successfully decoding both sensors' packets is slightly higher than $(p^{\mathrm{N}})^2$.

Comparing TDMA-CDRT and NOMA-CDRT, as shown in Fig. 6(a), the average peak AoI of the direct sensor is significantly lower in NOMA-CDRT than in TDMA-CDRT. This is because the direct sensor sends one update packet per time slot in NOMA-CDRT, while it sends one update packet per three time slots in TDMA-CDRT. Although NOMA reduces the successful reception probability due to wireless interference, sending update packets more frequently in NOMA-CDRT could still lower the average peak AoI of the direct sensor. In contrast, Fig. 6(b) shows that the average peak AoI performance of the relay-aided sensor in NOMA-CDRT is worse than that in TDMA-CDRT in the low to medium SNR regime. Although the relay-aided sensor also has a higher frequency of sending update packets in NOMA-CDRT, its average peak AoI is higher than that of TDMA-CDRT due to the lower successful probability of NOMA decoding. In each hop of NOMA-CDRT, the packet of the relay-aided sensor interferes with that from the direct sensor. Since the direct sensor prefers NOMA-CDRT while the relay-aided sensor prefers TDMA-CDRT, Fig. 6(c) shows the average peak AoI of the entire CDRT system, where TDMA-CDRT outperforms NOMA-CDRT in the low to medium SNR regime. As the SNR increases, NOMA-CDRT gradually outperforms TDMA-CDRT, because the successful reception probabilities also increase and NOMA allows both sensors to transmit sensed data more frequently.

Fig. 6 shows that TDMA-CDRT and NOMA-CDRT are not superior to each other. Both schemes are beneficial for either of the sensors and have their unfavorable SNR regimes. By contrast, our hybrid CDRT scheme (NOMA-OMA-CDRT and OMA-NOMA-CDRT) balances the needs of the direct and relay-aided sensors. Unlike TDMA-CDRT and NOMA-CDRT, the hybrid CDRT scheme maintains a relatively low average peak AoI for both sensors as well as for the whole system. In particular, the relay-aided sensor in the hybrid CDRT scheme has the best average peak AoI performance in the moderate SNR regime. The hybrid CDRT reduces the time interval of consecutive transmissions without significantly compromising the successful reception probability of update packets.

The above experiments assume that the links in CDRT have the same SNR. However, in time-varying wireless environments, these links are more likely to have different

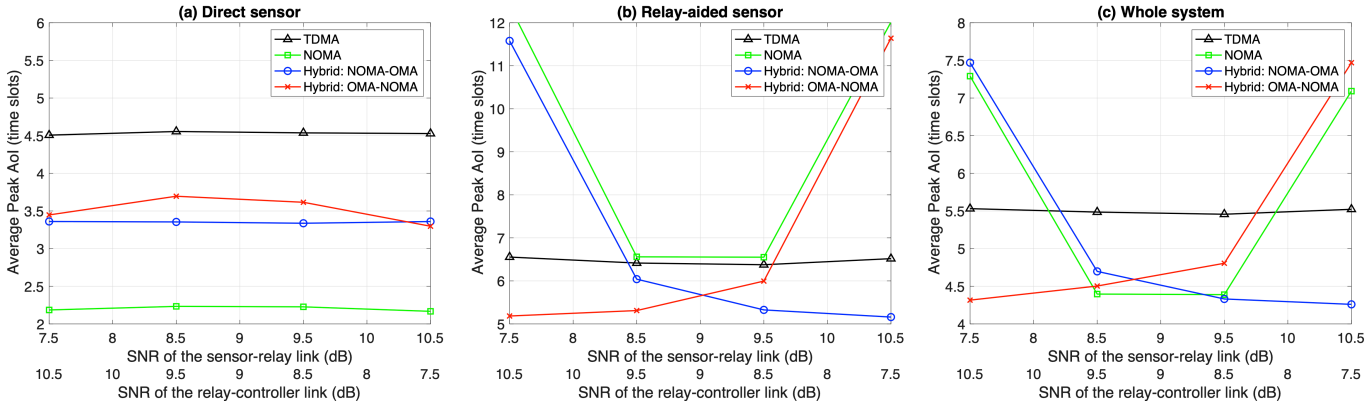


Fig. 7. SDR experimental results for the average peak AoI of (a) the direct sensor, (b) the relay-aided sensor, and (c) the whole system under different CDRT schemes with the SNR-imbalanced scenario, where the SNR from the direct sensor to the controller and the relay in (a)–(c) are fixed at 9.5 dB.

channel conditions. We now investigate the average peak AoI performance when the links have different SNRs, i.e., the SNR-imbalanced scenario, as illustrated in Figs. 7(a)–(c). We fix the SNR of the direct sensor to 9.5 dB at the controller and the relay. Then, we vary the SNR from the relay-aided sensor to the relay from 7.5 dB to 10.5 dB while that from the relay to the controller from 10.5 dB to 7.5 dB. The different SNR pairs are set to simulate different relay locations or different transmit powers of the nodes.

Fig. 7(a) shows that the direct sensor has similar AoI performance in the SNR-imbalanced and SNR-balanced cases, e.g., it prefers NOMA-CDRT. Nevertheless, Fig. 7(b) shows that the relay-aided sensor has different results in the SNR-imbalanced case. The average peak AoI of the relay-aided sensor is much higher in NOMA-CDRT than in TDMA-CDRT. The reason is apparent: the update is unsuccessful if the packet of the relay-aided sensor is corrupted in any hop, which easily happens in the SNR-imbalanced case because either hop has a low SNR. The controller has to wait longer to receive the next successful update. In contrast, the hybrid CDRT scheme outperforms TDMA-CDRT and NOMA-CDRT in the SNR-imbalanced scenario. For example, NOMA-OMA-CDRT achieves the best AoI performance under a poor relay-controller link, because the direct sensor remains silent when the relay forwards the packet to the controller. Likewise, when the SNR from the relay-aided sensor to the relay is low, OMA-NOMA-CDRT outperforms other schemes.

Considering the average peak AoI performance of the whole system, Fig. 7(c) shows that NOMA-CDRT is significantly worse than TDMA-CDRT when the SNR of the sensor-relay or relay-controller link is poor. Furthermore, the hybrid CDRT scheme outperforms NOMA-CDRT and TDMA-CDRT in average peak AoI. The performance gain is significant when the relay-aided sensor has a lower SNR in either hop, because an interference-free channel is assigned to the hop with lower SNR for better decoding performance.

To conclude, the hybrid CDRT scheme strikes a balance between the needs of the relay-aided and direct sensors, both of which convey critical information updates. More importantly, when the links in CDRT have different SNRs, the hybrid CDRT scheme outperforms conventional TDMA-CDRT and NOMA-CDRT schemes. We can choose to employ NOMA-OMA-CDRT or OMA-NOMA-CDRT depending on the actual situation. For example, when the transmit power of the relay-aided sensor (e.g., a tiny sensor in the factory) is weak, so the received SNR at the relay is low, we can strategically use OMA-NOMA-CDRT to achieve the best average peak AoI performance. Hence, the hybrid CDRT scheme is a robust solution for deploying relay-assisted information update systems in the IoT.

## VI. Conclusion

We have investigated the average peak AoI of different CDRT schemes for real-time status update. In particular, we put forth a hybrid CDRT scheme combining TDMA and NOMA and maintaining high information freshness for the whole CDRT system.

Information freshness is of paramount importance when a direct sensor and a relay-aided sensor send the sensed data to a common receiver for seamless monitoring. Our investigations on AoI reveal interesting findings for information update systems using CDRT. Specifically, our SDR experiments indicate that TDMA-CDRT and NOMA-CDRT do not outperform each other in terms of average peak AoI in all SNR regimes. In error-prone wireless networks, to achieve a low average peak AoI, the direct sensor prefers NOMA-CDRT, while the relay-aided sensor prefers TDMA-CDRT, thereby posing a dilemma in the optimization of the average peak AoI of CDRT networks.

To address the above dilemma, we design a hybrid CDRT scheme with two variations, namely NOMA-OMA-CDRT and OMA-NOMA-CDRT. Experiments show that the hybrid CDRT scheme can balance the average peak AoI of the direct and relay-aided sensors. Furthermore, unlike TDMA-CDRT and NOMA-CDRT, which have significantly worse average peak AoI performance under their respective unfavorable SNR regimes, the hybrid CDRT scheme can maintain a low average peak AoI of the whole CDRT system when the SNR varies. Overall, our hybrid CDRT scheme is a practical and promising solution for information update systems with AoI

requirements.

## APPENDIX A
## DERIVATION OF $\mathbb{E}[X_{\mathrm{d}}^{\mathrm{NO}}]$ IN NOMA-CDRT

We use the Markov model shown in Fig. 8 to derive $\mathbb{E}[X_{\mathrm{d}}^{\mathrm{NO}}]$. In the Markov model, states $\Omega = \{S^{(1)}, F^{(1)}, S^{(2)}, F^{(2)}\}$ represent the packet from the direct sensor being transmitted {successfully in the first time slot, unsuccessfully in the first time slot, successfully in the second time slot, unsuccessfully in the second time slot}, respectively.

Let $\mathbf{\Phi}$ be the state transition matrix that

$$\begin{aligned}\mathbf{\Phi} &= \begin{bmatrix} \varphi_{S^{(1)}S^{(1)}} & \varphi_{S^{(1)}F^{(1)}} & \varphi_{S^{(1)}S^{(2)}} & \varphi_{S^{(1)}F^{(2)}} \\ \varphi_{F^{(1)}S^{(1)}} & \varphi_{F^{(1)}F^{(1)}} & \varphi_{F^{(1)}S^{(2)}} & \varphi_{F^{(1)}F^{(2)}} \\ \varphi_{S^{(2)}S^{(1)}} & \varphi_{S^{(2)}F^{(1)}} & \varphi_{S^{(2)}S^{(2)}} & \varphi_{S^{(2)}F^{(2)}} \\ \varphi_{F^{(2)}S^{(1)}} & \varphi_{F^{(2)}F^{(1)}} & \varphi_{F^{(2)}S^{(2)}} & \varphi_{F^{(2)}F^{(2)}} \end{bmatrix} \\ &= \begin{bmatrix} 0 & 0 & P_{\mathrm{d},2}^{\mathrm{NO}} & 1-P_{\mathrm{d},2}^{\mathrm{NO}} \\ 0 & 0 & P_{\mathrm{d},2}^{\mathrm{NO}} & 1-P_{\mathrm{d},2}^{\mathrm{NO}} \\ P_{\mathrm{d},1}^{\mathrm{NO}} & 1-P_{\mathrm{d},1}^{\mathrm{NO}} & 0 & 0 \\ P_{\mathrm{d},1}^{\mathrm{NO}} & 1-P_{\mathrm{d},1}^{\mathrm{NO}} & 0 & 0 \end{bmatrix}, \end{aligned} \tag{14}$$

where $\varphi_{ij}$ is the transition probability from state $i$ to state $j$. $P_{\mathrm{d},1}^{\mathrm{NO}}$ and $P_{\mathrm{d},2}^{\mathrm{NO}}$ are the successful reception probabilities of the packet from the direct sensor to the controller in the first and second time slots, respectively. The stationary distribution $\Pi$ of the Markov model can be found by solving $\Pi = \Pi\mathbf{\Phi}$, i.e.,

$$\begin{aligned}\Pi &= [\pi_{S^{(1)}}, \pi_{F^{(1)}}, \pi_{S^{(2)}}, \pi_{F^{(2)}}] \\ &= \left[\frac{P_{\mathrm{d},1}^{\mathrm{NO}}}{2}, \frac{1-P_{\mathrm{d},1}^{\mathrm{NO}}}{2}, \frac{P_{\mathrm{d},2}^{\mathrm{NO}}}{2}, \frac{1-P_{\mathrm{d},2}^{\mathrm{NO}}}{2}\right]. \end{aligned} \tag{15}$$

We denote by $u_\alpha$ the average number of state transitions required to change from initial state $\alpha$ to state $S \in \{S^{(1)}, S^{(2)}\}$ for the first time, i.e.,

$$u_\alpha = \begin{cases} 0, & \alpha \in \{S^{(1)}, S^{(2)}\} \\ 1 + \sum_{i \in \{F^{(1)}, F^{(2)}\}} \varphi_{\alpha i} u_i, & \alpha \in \{F^{(1)}, F^{(2)}\} \end{cases}. \tag{16}$$

In other words, we have

$$\begin{cases} u_{S^{(1)}} &= 0, \\ u_{F^{(1)}} &= 1 + \varphi_{F^{(1)}F^{(2)}} u_{F^{(2)}}, \\ u_{S^{(2)}} &= 0, \\ u_{F^{(2)}} &= 1 + \varphi_{F^{(2)}F^{(1)}} u_{F^{(1)}}. \end{cases} \tag{17}$$

The expected value $\mathbb{E}[X_{\mathrm{d}}^{\mathrm{NO}}]$ is the average number of update packets transmitted by the direct sensor between two consecutive successful decodings at the controller. This means the average number of time slots required to depart from state $S \in \{S^{(1)}, S^{(2)}\}$ and then return to state $S \in \{S^{(1)}, S^{(2)}\}$ for the first time. Then we denoted by $w_{S^{(1)}}$ and $w_{S^{(2)}}$ the average number of time slots needed to leave states $S^{(1)}$ and $S^{(2)}$, respectively, and then return to state $S \in \{S^{(1)}, S^{(2)}\}$ for the first time. Thus, we have

$$\begin{cases} w_{S^{(1)}} = 1 + \sum_{j \in \Omega} \varphi_{S^{(1)}j} u_j = 1 + \varphi_{S^{(1)}F^{(2)}} u_{F^{(2)}}, \\ w_{S^{(2)}} = 1 + \sum_{j \in \Omega} \varphi_{S^{(2)}j} u_j = 1 + \varphi_{S^{(2)}F^{(1)}} u_{F^{(1)}}. \end{cases} \tag{18}$$

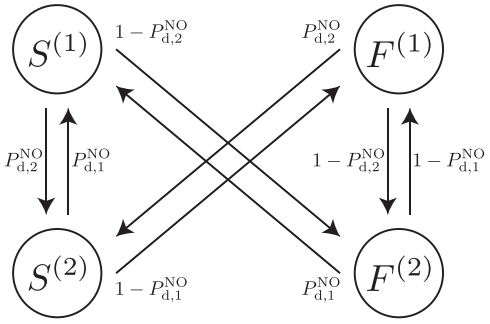


Fig. 8. The Markov model of NOMA-CDRT. States $\Omega = \{S^{(1)}, F^{(1)}, S^{(2)}, F^{(2)}\}$ represent the status in transmission, i.e., the packet from the direct sensor is transmitted {successfully in the first time slot, unsuccessfully in the first time slot, successfully in the second time slot, unsuccessfully in the second time slot}, respectively.

Solving (17) and (18), we get

$$\begin{cases} w_{S^{(1)}} = \frac{2-P_{\mathrm{d},2}^{\mathrm{NO}}}{P_{\mathrm{d},1}^{\mathrm{NO}}+P_{\mathrm{d},2}^{\mathrm{NO}}-P_{\mathrm{d},1}^{\mathrm{NO}}P_{\mathrm{d},2}^{\mathrm{NO}}}, \\ w_{S^{(2)}} = \frac{2-P_{\mathrm{d},1}^{\mathrm{NO}}}{P_{\mathrm{d},1}^{\mathrm{NO}}+P_{\mathrm{d},2}^{\mathrm{NO}}-P_{\mathrm{d},1}^{\mathrm{NO}}P_{\mathrm{d},2}^{\mathrm{NO}}}. \end{cases} \tag{19}$$

Finally, the proportion of states, $S^{(1)}$ and $S^{(2)}$, in the successful decoding can be found using the stationary distribution of the Markov model. Therefore, the average number of update packets transmitted by the direct sensor between two consecutive successful decodings at the controller is

$$\begin{aligned}\mathbb{E}[X_{\mathrm{d}}^{\mathrm{NO}}] &= \frac{\pi_{S^{(1)}}}{\pi_{S^{(1)}}+\pi_{S^{(2)}}} w_{S^{(1)}} + \frac{\pi_{S^{(2)}}}{\pi_{S^{(1)}}+\pi_{S^{(2)}}} w_{S^{(2)}} \\ &= \frac{2}{P_{\mathrm{d},1}^{\mathrm{NO}}+P_{\mathrm{d},2}^{\mathrm{NO}}}. \end{aligned} \tag{20}$$

## APPENDIX B
## AVERAGE PEAK AOI OF OMA-NOMA-CDRT

The idea of OMA-NOMA-CDRT is similar to NOMA-OMA-CDRT described in Section IV. The main difference is that OMA-NOMA-CDRT starts with OMA followed by NOMA, as shown in Fig. 9. In the first time slot, only the relay-aided sensor sends its packet to the relay, while the direct sensor remains silent. In the second time slot, if the decoding is successful, the relay forwards the packet to the controller. Meanwhile, the direct sensor also conveys its packet to the controller regardless of whether the relay transmits.

Although the two variations (NOMA-OMA-CDRT and OMA-NOMA-CDRT) are conceptually similar, their AoI performance differs due to the different successful reception probabilities of the packet at the nodes. In this appendix, to avoid repetition, we only highlight the important differences in the successful reception probability of the direct sensor for the two variations.

In the first hop, the successful reception probability of the packet from the relay-aided sensor to the relay is $P_{\mathrm{r1}}^{\text{O-NO}} = p^{\mathrm{O}}$ because of the absence of interference. Considering the second hop, there are two possible cases:

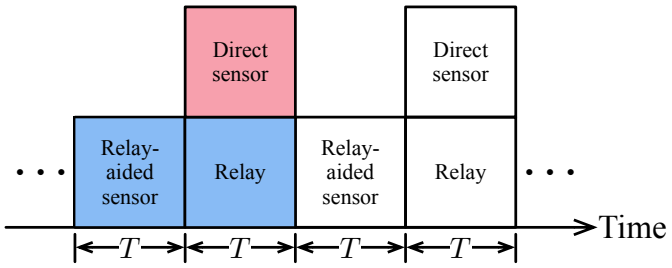


Fig. 9. OMA-NOMA-CDRT system model.

- Case I, with probability $P_{\mathrm{r1}}^{\text{O-NO}}$: since the packet from the relay-aided sensor is successfully decoded at the relay in the first time slot, the packets from the relay and the direct sensor interfere with each other at the controller in the second hop. Therefore, due to the use of NOMA decoding, the successful reception probability of the packets from the relay ($P_{\mathrm{r2}}^{\text{O-NO}}$) and the direct sensor ($P_{\mathrm{d,1}}^{\text{O-NO}}$) to the controller in the second hop are $p^{\mathrm{N}}$.
- Case II, with probability $(1 - P_{\mathrm{r1}}^{\text{O-NO}})$: since the packet from the relay-aided sensor fails to be decoded at the relay in the first time slot, only the direct sensor transmits its packet in the second time slot with successful reception probability $P_{\mathrm{d,2}}^{\text{O-NO}} = p^{\mathrm{O}}$.

Therefore, the overall successful reception probability of the packet from the direct sensor is

$$\begin{aligned} P_{\mathrm{d}}^{\text{O-NO}} &= P_{\mathrm{r1}}^{\text{O-NO}}(P_{\mathrm{d,1}}^{\text{O-NO}}) + (1 - P_{\mathrm{r1}}^{\text{O-NO}})P_{\mathrm{d,2}}^{\text{O-NO}} \\ &= p^{\mathrm{O}}p^{\mathrm{N}} + (1 - p^{\mathrm{O}})p^{\mathrm{O}}, \end{aligned} \tag{21}$$

while that of the packet from the relay-aided sensor is

$$P_{\mathrm{r}}^{\text{O-NO}} = P_{\mathrm{r1}}^{\text{O-NO}}P_{\mathrm{r2}}^{\text{O-NO}} = p^{\mathrm{O}}p^{\mathrm{N}}. \tag{22}$$

As in Section IV, the average peak AoI of the direct sensor is computed by

$$\overline{\Delta}_{\mathrm{d}}^{\text{O-NO}} = \mathbb{E}[\tau_{\mathrm{d}}^{\text{O-NO}}] + \mathbb{E}[Z_{\mathrm{d}}^{\text{O-NO}}] = T\left(\frac{2}{p^{\mathrm{O}} + p^{\mathrm{O}}p^{\mathrm{N}} - (p^{\mathrm{O}})^2} + 1\right), \tag{23}$$

and the average peak AoI of the relay-aided sensor is computed by

$$\overline{\Delta}_{\mathrm{r}}^{\text{O-NO}} = \mathbb{E}[\tau_{\mathrm{r}}^{\text{O-NO}}] + \mathbb{E}[Z_{\mathrm{r}}^{\text{O-NO}}] = T\left(\frac{2}{p^{\mathrm{O}}p^{\mathrm{N}}} + 2\right). \tag{24}$$

Finally, the average peak AoI of the whole system is

$$\begin{aligned} \overline{\Delta}^{\text{O-NO}} &= \frac{1}{2}\left(\overline{\Delta}_{\mathrm{d}}^{\text{O-NO}} + \overline{\Delta}_{\mathrm{r}}^{\text{O-NO}}\right) \\ &= \frac{1}{2}\left(T\left(\frac{2}{p^{\mathrm{O}} + p^{\mathrm{O}}p^{\mathrm{N}} - (p^{\mathrm{O}})^2} + 1\right) + T\left(\frac{2}{p^{\mathrm{O}}p^{\mathrm{N}}} + 2\right)\right) \\ &= T\left(\frac{1}{p^{\mathrm{O}} + p^{\mathrm{O}}p^{\mathrm{B}} - (p^{\mathrm{O}})^2} + \frac{1}{p^{\mathrm{O}}p^{\mathrm{N}}} + \frac{3}{2}\right). \end{aligned} \tag{25}$$

## REFERENCES


[1] M. A. Abd-Elmagid, N. Pappas, and H. S. Dhillon, "On the role of age of information in the Internet of things," *IEEE Commun. Mag.*, vol. 57, no. 12, pp. 72–77, Dec. 2019.

[2] H. Xu, W. Yu, D. Griffith, and N. Golmie, "A survey on industrial Internet of things: A cyber-physical systems perspective," *IEEE Access*, vol. 6, pp. 78238–78259, Dec. 2018.

[3] U. Uyoata, J. Mwangama, and R. Adeogun, "Relaying in the Internet of things (IoT): A survey," *IEEE Access*, vol. 9, pp. 132675–132704, Sep. 2021.

[4] C. Thai and P. Popovski, "Coordinated direct and relay transmission with interference cancelation in wireless systems," *IEEE Commun. Lett.*, vol. 15, no. 4, pp. 416–418, Apr. 2011.

[5] T.-T. Chan, H. Pan, and J. Liang, "Age of information with joint packet coding in industrial IoT," *IEEE Wireless Commun. Lett.*, vol. 10, no. 11, pp. 2499–2503, Nov. 2021.

[6] S. Kaul, M. Gruteser, V. Rai, and J. Kenney, "Minimizing age of information in vehicular networks," in *Proc. IEEE Int. Conf. Sens., Commun. Netw.*, Jun. 2011.

[7] S. Kaul, R. Yates, and M. Gruteser, "Real-time status: How often should one update?," in *Proc. IEEE INFOCOM*, Mar. 2012.

[8] A. Kosta, N. Pappas, and V. Angelakis, "Age of information: A new concept, metric, and tool," *Found. Trends Netw.*, vol. 12, no. 3, pp. 162–259, Nov. 2017.

[9] A. M. Bedewy, Y. Sun, and N. B. Shroff, "Minimizing the age of information through queues," *IEEE Trans. Inf. Theory*, vol. 65, no. 8, pp. 5215–5232, Aug. 2019.

[10] Y. Inoue, H. Masuyama, T. Takine, and T. Tanaka, "A general formula for the stationary distribution of the age of information and its application to single-server queues," *IEEE Trans. Inf. Theory*, vol. 65, no. 12, pp. 8305–8324, Dec. 2019.

[11] L. Corneo, C. Rohner, and P. Gunningberg, "Age of information-aware scheduling for timely and scalable Internet of things applications," in *Proc. IEEE INFOCOM*, Jun. 2019.

[12] D. Sinha and R. Roy, "Deadline-aware scheduling for maximizing information freshness in industrial cyber-physical system," *IEEE Sensors J.*, vol. 21, no. 1, pp. 381–393, Jan. 2021.

[13] V. W. Håkansson, N. K. D. Venkategowda, S. Werner, and P. K. Varshney, "Optimal transmission-constrained scheduling of spatio-temporally dependent observations using age-of-information," *IEEE Sensors J.*, early access, Jul. 2022.

[14] R. D. Yates *et al.*, "Age of information: An introduction and survey," *IEEE J. Sel. Areas Commun.*, vol. 39, no. 5, pp. 1183–1210, May 2021.

[15] S. M. R. Islam, N. Avazov, O. A. Dobre, and K.-S. Kwak, "Power-domain non-orthogonal multiple access (NOMA) in 5G systems: Potentials and challenges," *IEEE Commun. Surveys Tuts.*, vol. 19, no. 2, pp. 721–742, 2nd Quart., 2017.

[16] Z. Ding *et al.*, "A survey on non-orthogonal multiple access for 5G networks: Research challenges and future trends," *IEEE J. Select. Areas Commun.*, vol. 35, no. 10, pp. 2181–2195, Oct. 2017.

[17] J.-B. Kim and I.-H. Lee, "Non-orthogonal multiple access in coordinated direct and relay transmission," *IEEE Commun. Lett.*, vol. 19, no. 11, pp. 2037–2040, Nov. 2015.

[18] M. F. Kader and S. Y. Shin, "Coordinated direct and relay transmission using uplink NOMA," *IEEE Wireless Commun. Lett.*, vol. 7, no. 3, pp. 400–403, Jun. 2018.

[19] M. Yang *et al.*, "Design and performance analysis of cooperative NOMA with coordinated direct and relay transmission," *IEEE Access*, vol. 7, pp. 73306–73323, 2019.

[20] X. Pei *et al.*, "NOMA-based coordinated direct and relay transmission with a half-duplex/full-duplex relay," *IEEE Trans. Commun.*, vol. 68, no. 11, pp. 6750–6760, Nov. 2020.

[21] H. Pan, J. Liang, and S. C. Liew, "Practical NOMA-based coordinated direct and relay transmission," *IEEE Wireless Commun. Lett.*, vol. 10, no. 1, pp. 170–174, Jan. 2021.

[22] Y. Xu *et al.*, "Coordinated direct and relay transmission with NOMA and network coding in Nakagami-m fading channels," *IEEE Trans. Commun.*, vol. 69, no. 1, pp. 207–222, Jan. 2021.

[23] H. Pan, J. Liang, S. C. Liew, V. C. M. Leung, and J. Li, "Timely information update with nonorthogonal multiple access," *IEEE Trans. Ind. Inform.*, vol. 17, no. 6, pp. 4096–4106, Jun. 2021.

[24] Ettus Inc., "Universal software radio peripheral," [Online]. Available: https://www.ettus.com/. Accessed on: Jul. 1, 2022.

[25] G. FSF, "GNU Radio—GNU FSF Project," [Online]. Available: http://gnuradio.org/redmine/wiki/gnuradio. Accessed on: Jul. 1, 2022.

[26] H. Pan and S. C. Liew, "Backbone-assisted wireless local area network," *IEEE Trans. Mobile Comput.*, vol. 20, no. 3, pp. 830–845, Mar. 2021.

**Tse-Tin Chan** (S'16-M'20) received his B. Eng. (First Class Honours) and Ph.D. in Information Engineering from the Chinese University of Hong Kong (CUHK) in 2014 and 2020, respectively. He is currently an Assistant Professor in the Department of Mathematics and Information Technology at the Education University of Hong Kong (EdUHK). Before that, he was an Assistant Professor in the Department of Computing at the Hang Seng University of Hong Kong (HSUHK) from 2020 to 2022. His research interests include wireless communications and networking, Internet of things (IoT), age of information (AoI), and machine learning for communications.

**Haoyuan Pan** (S'16-M'19) received the B.E. and Ph.D. degrees in Information Engineering from The Chinese University of Hong Kong (CUHK), Hong Kong, in 2014 and 2018, respectively. He was a Post-Doctoral Fellow with the Department of Information Engineering, CUHK, from 2018 to 2020. He is currently an Assistant Professor with the College of Computer Science and Software Engineering, Shenzhen University, Shenzhen, China. His research interests include wireless communications and networks, Internet of things (IoT), semantic communications, and age of information (AoI).